Bosons, gauge fields, and high-T_c cuprates

Don H. Kim, Derek K. K. Lee, and Patrick A. Lee
Department of Physics, Massachussetts Institute of Technology, Cambridge, Massachusetts 02139
(Received 22 July 1996)

A simple model of a degenerate two-dimensional Bose liquid interacting with a fluctuating gauge field is investigated as a possible candidate to describe the charge degree of freedom in the normal state of the cuprate superconductors. We show that the fluctuating gauge field efficiently destroys superfluidity even in the Bose degenerate regime. We discuss the nature of the resulting normal state in terms of the geometric properties of the imaginary-time paths of the bosons. We will also present numerical results on the transport properties and the density correlations in the system. We find a transport scattering rate of $\hbar/\tau_{\rm tr} \sim 2k_BT$, consistent with the experiments on the cuprates in the normal state. We also find that the density correlations of our model resemble the charge correlations of the *t-J* model. [S0163-1829(97)08601-3]

We study the low-temperature behavior of repulsive bosons in a spatially fluctuating gauge field in two dimensions. This is motivated by the gauge theories of the *t-J* model for the cuprate superconductors, where low-energy charge excitations are described by bosonic degrees of freedom. The internal gauge field of this model suppresses superfluidity in the Bose liquid, even below the Bose degeneracy temperature when there is significant exchange among the bosons. We can study the imaginary-time trajectories of the bosons in the path-integral representation of this model. We see that the boson world lines retrace themselves in the presence of strong gauge fluctuations, giving rise to interesting dynamics in this degenerate but metallic Bose liquid.

We have studied this metallic state using quantum Monte Carlo techniques. We find that this model does indeed capture some of the long-wavelength charge properties which are common to the cuprate superconductors. This includes a linear temperature dependence of the transport scattering rate $1/\tau_{\rm tr}$, as deduced from a Drude-like optical conductivity from our model. This is consistent with experimental data on the cuprate superconductors near optimal doping. We also find that the density excitations in our model are qualitatively similar to those in the full *t-J* model, by comparing our results with diagonalization results in the literature. A brief account of this work has already appeared.[1]

I. MOTIVATION

The normal metallic state of the superconducting cuprates displays many non-Fermi-liquid properties. For instance, the in-plane resistivity of $La_{2-x}Sr_xCuO_4$ has a power-law temperature dependence of the form $\rho \propto T^{\alpha}$ where α increases from 1 to 1.5 with increasing hole doping.[2] In particular, near optimal doping, the resistivity is linear in temperature up to 1000 K. This linear-T dependence is found in many of the cuprate superconductors with similar values of $d\rho/dT$ (1.2 $\mu\Omega$ cm/K $\pm$ 20%).[3] This should be contrasted with the quadratic temperature dependence of Fermi-liquid theory. Similarly, the transport relaxation rate appears to be universal among optimally doped compounds: $1/\tau_{\rm tr} \simeq 2k_BT$ [from a two-component-model analysis of the optical conductivity in YBCO,[4] LSCO,[5] Bi2212,[6] Bi2201 (Ref. 6)]. Transport in a magnetic field is also anomalous. The Hall coefficient indicates the existence of holelike carriers in the doping range where superconductivity occurs. The Hall coefficient R_H increases with decreasing temperature, but it remains smaller than the classical value of $1/n_hec$ for a hole density of n_h for a wide range of temperatures down to the superconducting transition. These compounds also have a small positive magnetoresistance with a temperature dependence[7] different from conventional theory using $\tau_{\rm tr}$.

The transport properties of these compounds appear to have common features in spite of considerable differences in the transition temperature and spin fluctuation properties among these compounds. This indicates that a common mechanism is responsible for the scattering of charge carriers in these materials. One might hope that this scattering mechanism can be understood in terms of a low-energy theory with a minimum number of microscopic parameters. In this paper, we study a Bose liquid in a fluctuating gauge field as a possible candidate for such an effective theory.

The anomalous transport behavior, together with other unusual features such as temperature-dependent magnetic susceptibility and non-Korringa behavior of the nuclear magnetic relaxation time, leads to the conclusion that the metallic state of the cuprates cannot be described in a simple Fermi-liquid scenario. It has been postulated that ''spin-charge separation'' is responsible for these anomalies.[8] For instance, such a scenario might reconcile the apparent low density and holelike character of the charge carriers with the observation of a large, electronlike Fermi surface in photoemission. Numerical studies of the *t-J* model, which is believed to be a low-energy model of the cuprates, also provide some support for spin-charge separation,[9–11] such as different energy scales for the spin and charge excitations, and the suppression of $2k_F$ scattering in the charge spectrum.

A model of spin-charge separation is a gauge theory where neutral spin-half fermions (''spinons'') and charge-e bosons (''holons'') interact via an internal $U(1)$ gauge field.[12,13] Physically, the transverse part of the gauge field is related to ''spin chirality'' fluctuations.[13] In this picture, the charge properties of the system should be dominated by the behavior of the holons. We will study the holon subsystem in

this paper, treating the spinon subsystem simply as a medium through which the gauge field propagates. To be more precise, we study a model of bosons with on-site repulsion in the presence of a spatially fluctuating magnetic field with short-range correlations. The repulsive interaction is necessary for the stability of the system, which means that one cannot treat this problem perturbatively starting from an ideal Bose gas. Previous studies[14–18] have implicitly studied the nondegenerate regime of low density or high temperature, whereas the regime relevant to the cuprates is the degenerate regime where the thermal de Broglie wavelength of the bosons is greater than the mean particle spacing. A concern from earlier studies of the gauge model is that degenerate bosons would have strong diamagnetic response to the internal gauge field and hence effectively Bose-condense at a relatively high temperature ($k_B T_{BE} \sim 4\pi n_h t \sim 1000$ K). This would in fact restore Fermi-liquid behavior to the system. We shall show here that gauge fluctuations suppress this diamagnetic response and the bosons remain normal without strong diamagnetism at all finite temperatures. Furthermore, our numerical results indicate that the resistivity of this Bose metallic phase has a linear temperature dependence which is consistent with experiments.

It should be noted that we will work exclusively in the ''slave-boson'' scheme where the holons are bosonic and the spinons are fermionic. One may also obtain a ''slave-fermion'' gauge theory where the statistics of the holons and spinons are interchanged. Although these two approaches are equivalent in principle, they do not produce the same results in treatments which consider only Gaussian fluctuations around a mean-field solution. We believe that, at this level of approximation, the slave-boson approach provides a better starting point to describe the cuprates near optimal doping (for instance, the observation of a large Fermi surface in photoemission), while the slave-fermion theory may be more suitable near an antiferromagnetic state at very low doping. The physics of the spin gap in the underdoped regime is also beyond the scope of the $U(1)$ gauge theory described in this work (see Ref. 19).

Besides the possible relevance to the transport in the cuprate superconductors, the model we consider is of intrinsic theoretical interest. The model is a Bose version of the problem of a quantum particle in a random magnetic flux, which has received considerable attention in recent years. It is also related to frustrated spin systems and vortex glasses. However, since we deal exclusively with annealed averaging in this paper (see below), we cannot draw any direct conclusions about these problems with quenched disorder.

The rest of the paper is organized as follows. In Sec. II, we review the connection between the gauge theory of the *t-J* model and our boson model. In Sec. III, we discuss the path-integral formalism which provides a convenient framework to visualize physical processes in terms of the imaginary-time paths of the bosons. In Sec. IV, we look at the effects of the gauge field on the world-line geometry of the bosons. We will see that the partition function of the system is dominated by self-retracing world-line configurations. We will also argue that superfluidity is destroyed by the fluctuating gauge field, giving rise to a degenerate Bose metal. In the subsequent sections, we present the results of a quantum Monte Carlo study of this metallic phase. We will discuss the transport properties and the density correlations in this boson model.

II. BOSON GAUGE MODEL

In this section, we provide the motivation for studying an effective boson model from the gauge theory of the *t-J* model, which describes the motion of vacancies in a doped Mott insulator:

$$\mathcal{H} = -t_0 \sum_{\langle ij\rangle \sigma} (c_{i\sigma}^\dagger c_{j\sigma} + \text{H.c.}) + J \sum_{\langle ij\rangle} \mathbf{S}_i \cdot \mathbf{S}_j \tag{1}$$

with the constraint of no double occupancy. Experimentally, $J \simeq 1500$ K and $t_0/J \simeq 3$.

The constraint of no double occupancy allows us to write the creation of a physical hole in terms of the creation of a charged hard-core boson (holon) and the annihilation of a spin-half fermion (spinon): $c_{i\sigma} = f_{i\sigma} b_i^\dagger$ In terms of these slave bosons and fermions, the Hamiltonian of the *t-J* model can be written as:

$$\mathcal{H} = -t_0 \sum_{\langle ij\rangle \sigma} (f_{i\sigma}^\dagger b_i b_j^\dagger f_{j\sigma} + \text{H.c.}) + J \sum_{\langle ij\rangle} \mathbf{S}_i \cdot \mathbf{S}_j + \sum_i i a_{0i} (f_{i\sigma}^\dagger f_{i\sigma} + b_i^\dagger b_i - 1), \tag{2}$$

where $\mathbf{S}_i = f_{i\alpha}^\dagger \sigma_{\alpha\beta} f_{i\beta}$, The a_{0i} field is a Lagrange multiplier enforcing the local occupancy constraint, and acts as a fluctuating scalar potential for the spinons and holons.

Among the mean-field theories proposed to decouple the quartic terms in Eq. (2), a candidate for the normal state near optimal doping is the the uniform resonating-valence-bond (RVB) ansatz: $\Sigma_\sigma \langle f_{i\sigma}^\dagger f_{j\sigma}\rangle = \xi e^{i a_{ij}}$. This incorporates short-range antiferromagnetic correlations without any long-range Néel order. The Lagrangian of this RVB phase can be written as:

$$\mathcal{L} = \sum_{i,\sigma} f_{i\sigma}^* (\partial_\tau - \mu_F + i a_{0i}) f_{i\sigma} + \sum_i b_i^* (\partial_\tau - \mu_B + i a_{0i}) b_i - \frac{J}{2} \xi \sum_{\langle ij\rangle} (e^{i a_{ij}} f_{i\sigma}^* f_{j\sigma} + \text{H.c.}) - t_0 \xi \sum_{\langle ij\rangle} (e^{i a_{ij}} b_i^* b_j + \text{H.c.}). \tag{3}$$

The vector potential a_{ij} arises from the fluctuations in the phase of the RVB order parameter. Longitudinal fluctuations of the gauge field a_{ij} do not affect the Lagrangian due to an internal $U(1)$ gauge symmetry:

$$f_i \to f_i e^{i\theta_i}, \quad b_i \to b_i e^{i\theta_i}, \quad a_{ij} \to a_{ij} - \theta_i + \theta_j. \tag{4}$$

We will therefore work in a fixed gauge, such as the Coulomb gauge, and consider only the fluctuations in the transverse part of the gauge field a_{ij}. In other words, we will consider only fluctuations in the internal magnetic and electric fields which are gauge-invariant quantities.

Since we are interested in the charge degrees of freedom, we wish to consider an effective theory with bosons only, and regard the spinon fluid as a medium through which the gauge field propagates. The gauge field has no dynamics *in vacuo*. The response of the spinon fluid to the gauge field is responsible for the dynamics of the gauge field as seen by the holons. More specifically, we can obtain the Gaussian fluctuations of the a fields by treating the spinon response in the random-phase approximation. The effective gauge-field propagator is

$$\mathcal{S}_G=\frac{1}{2\beta L^2}\sum_{\mathbf{k},\omega_n}\Pi^{00}(\mathbf{k},\omega_n)a_0^*(\mathbf{k},\omega_n)a_0(\mathbf{k},\omega_n)$$
$$+\frac{1}{2\beta L^2}\sum_{\mathbf{k},\omega_n}\Pi^{\perp}(\mathbf{k},\omega_n)a_\perp^*(\mathbf{k},\omega_n)a_\perp(\mathbf{k},\omega_n), \quad (5)$$

where $\beta=1/T$, $\omega_n=2\pi nT$, L is the linear size of the system, and $a_\perp$ is the transverse part of the gauge field. (We use units where distance is measured in terms of the lattice spacing and $k_B=\hbar=e=1$.) Here, for small k and ω_n, $\Pi^{00}\simeq\rho_F$, the spinon density of states at the Fermi level. This describes the Thomas-Fermi screening of internal electric fields by the fermions. The effective interaction mediated by the screened a_0 field is a repulsion between the bosons (of range $\propto\rho_F^{-1/2}$), consistent with the original hard-core requirement for the bosons. We will model this with an on-site repulsion energy, U. On the other hand, the magnetic fields due to fluctuations in a_{ij} are not effectively screened out by the fermions.[20] The gauge-field fluctuations as experienced by the holons are therefore strong. More specifically, the Gaussian fluctuations have the correlation function $D(\mathbf{k},\omega_n)=\langle a_\perp^*(\mathbf{k},\omega_n)a_\perp(\mathbf{k},\omega_n)\rangle$, given (in the continuum limit) by

$$D(\mathbf{k},\omega_n)=\frac{1}{\Pi_\perp(\mathbf{k},\omega_n)}=\frac{1}{\gamma|\omega_n|/k+\chi k^2}, \quad (6)$$

where χ is the orbital susceptibility of the spinon fluid and γ is a Landau damping coefficient. (In units where the lattice spacing is unity, $\gamma\simeq\pi^2$ for a spinon gas near half-filling.) These gauge-field fluctuations cause profuse forward scattering of the bosons. We believe that this is the dominant scattering mechanism in this problem. Since it is overdamped at long wavelengths with a relaxation rate which diverges as $1/k^3$, we will ignore the slow relaxation and work in a ''quasistatic'' limit for the gauge fields:

$$D(\mathbf{k},\omega_n)\to D(\mathbf{k},\omega_n=0)\,\delta_{n,0}=\delta_{n,0}/\chi k^2. \quad (7)$$

[On a square lattice, k^2 is replaced by $4-2(\cos k_x+\cos k_y)$.] This quasistatic approximation is justified when the gauge field relaxes on a time scale longer than $1/T$. In the Bose degenerate regime, the shortest scattering length of interest is the interparticle spacing of the bosons. The relevant relaxation time scales as $n_b^{3/2}\chi/\gamma$. For a spinon band with hopping J near half-filling, χ is a small fraction ($\sim 10^{-2}$) of J due to the weak diamagnetism of a Fermi system. One might therefore expect that this quasistatic approximation to be valid for temperatures down to a small fraction of J, i.e., for the whole of the normal state ($T>T_c\simeq 0.1J$).

One might object that arguments above are based on a weak-coupling theory of the response of the spinons to the gauge fields. However, we believe that the essential features remain correct in general, namely, a separation of times scales between the relaxation of the gauge fields and the boson dynamics, as well as the magnitude of the gauge fluctuations being controlled by the spinon diamagnetic susceptibility χ.

The gauge-field correlator (7) corresponds to a spatially uncorrelated flux distribution with the correlation function:

$$\langle\Phi_{\mathbf{r}}\Phi_{\mathbf{r}'}\rangle=\frac{T}{\chi}\delta_{\mathbf{r},\mathbf{r}'}, \quad (8)$$

where $\Phi_{\mathbf{r}}=(\Phi_0/2\pi)\Sigma_{\square}a_{ij}$ (oriented sum around the links of plaquette **r**) is the flux through plaquette **r**. ($\Phi_0=hc/e$ is the flux quantum.) Since we are treating the thermodynamics for the gauge field classically, we have a thermal factor of T in Eq. (8) for the flux variance $\langle\Phi^2\rangle$. Given that the fermion orbital susceptibility is roughly constant at low temperatures, we might expect the flux variance to have a linear temperature dependence. However, a lattice calculation by Hlubina *et al.*[21] has indicated that the Gaussian fluctuations are sufficiently strong that the flux through a plaquette is of the order of the flux quantum Φ_0: $\langle\Phi^2\rangle^{1/2}\geqslant 0.5\Phi_0$ down to a temperature of $0.4J$. Since the experimental superconducting T_c is of the order of $0.1J$, we expect that this regime of strong random flux is relevant to the normal state of the cuprates until one approaches the superconducting transition. In this regime, the precise value of $\langle\Phi^2\rangle$ should not affect the behavior of the bosons, and we will focus on a *large and temperature-independent* flux variance when we study the transport and correlation functions of our boson system.

Another factor leading to the reduction of the flux variance at low temperature is one that has not been discussed so far, namely, that the magnitude of the gauge field should also be affected by the diamagnetic response of the holons as well as the spinons, i.e., $\langle\Phi^2\rangle=T/[\chi_{\text{spinon}}(T)+\chi_{\text{holon}}(T)]$. The holon contribution dominates near an instability to Bose condensation where χ_{holon} diverges and the bosons develop a Meissner response to expel the gauge field from the system altogether. However, we will see in this paper that Bose condensation and the holon diamagnetism are strongly suppressed even below the boson degeneracy temperature. Therefore, in a wide range of temperatures above the superconducting T_c, we are justified in neglecting this feedback effect of the holons on the magnitude of the gauge-field fluctuations.

We can now define more precisely the effective model which we study in the rest of the paper. It is a model of lattice bosons interacting with a quasistatic gauge field, described by the effective action $S=S_B+S_G$:

$$S_B=\int_0^\beta\left(\sum_i b_i^*(\partial_\tau-\mu_B)b_i-H_B(\tau)\right)d\tau,$$

$$S_G=\frac{1}{2\beta L^2}\sum_{\mathbf{k}}D^{-1}(\mathbf{k},0)|a_\perp(\mathbf{k},0)|^2 \quad (9)$$

$$=\sum_{\mathbf{r}}\frac{\Phi_{\mathbf{r}}^2}{2\langle\Phi^2\rangle}, \quad (10)$$

with the boson Hamiltonian

$$H_B = -t\sum_{\langle ij\rangle} (e^{ia_{ij}} b_i^\dagger b_j + \text{H.c.}) + \frac{U}{2}\sum_i n_i(n_i-1), \quad (11)$$

where $t = t_0\xi \sim t_0$, L is the linear size in units of lattice spacing, and $U \gg t$. Note that, on performing the average over the gauge field, we average over static configurations only, i.e., $\mathbf{a}(\mathbf{k}, \omega_n \neq 0) = 0$.

We cannot say that we have rigorously derived above effective action from the slave-boson mean-field theory of the t-J model. Many approximations have been introduced to obtain this simple model with few adjustable parameters. For example, we have neglected the temperature dependence of the RVB order parameter ξ and also the gauge-field correlations of higher order.[22] We take the point of view that we are studying a ''minimal'' low-energy theory which hopefully captures many of the generic features of more complicated models.

III. PATH-INTEGRAL REPRESENTATION

It is convenient to study our boson model in a first-quantized formulation. The partition function Z for a system with N bosons in the canonical ensemble can be written in terms of a Feynman path integral[23] over the boson trajectories $\{\mathbf{x}_\alpha(\tau)\}$ $(\alpha = 1, \ldots, N)$:

$$Z = \frac{1}{N!}\sum_P \int^{\mathbf{x}(0)=P(\mathbf{x}(\beta))} \mathcal{D}[\mathbf{x}_1, \ldots, \mathbf{x}_N] \times \int \mathcal{D}\mathbf{a}\,\delta(\nabla\cdot\mathbf{a}) e^{-S_G(\mathbf{a}) - i\sum_\alpha \int_0^\beta \mathbf{a}\cdot\dot{\mathbf{x}}_\alpha d\tau - S_B^0(\{\mathbf{x}\})}, \quad (12)$$

where S_B^0 is the action for bosons in the absence of magnetic fields:

$$S_B^0 = \int_0^\beta d\tau \left(\sum_i b_i^* \partial_\tau b_i - H_B^0 \right), \quad (13)$$

where H_B^0 is given by Eq. (11) with $a_{ij} = 0$. In this section, we discuss the model in the continuum limit for notational convenience. In the continuum, one has

$$S_B^0 = \int_0^\beta d\tau \left[\sum_{\alpha=1}^N \frac{m}{2}\dot{\mathbf{x}}_\alpha^2 + \sum_{\alpha>\gamma} U\delta(\mathbf{x}_\alpha(\tau) - \mathbf{x}_\gamma(\tau)) \right]. \quad (14)$$

Particle identity is taken into account by performing the path integral over all trajectories where the set of final boson coordinates at $\{\mathbf{x}_1(\beta), \ldots, \mathbf{x}_N(\beta)\}$ is some permutation of the initial boson coordinates $\{\mathbf{x}_1(0), \ldots, \mathbf{x}_N(0)\}$. Any such permutations can be broken down to cycles. Each cycle forms a closed loop when the imaginary-time trajectories (world lines) of a many-boson configuration are projected onto real space. At high temperatures, cycles of length 1 dominate the partition function and the system is in a nondegenerate classical regime. At temperatures below the degeneracy temperature of the bosons, particles can travel large distances in the imaginary time, forming many ring exchanges (see Fig. 1).

In this formulation, we may integrate out the Gaussian fluctuations of the gauge field in Eq. (12). Thus, we arrive at

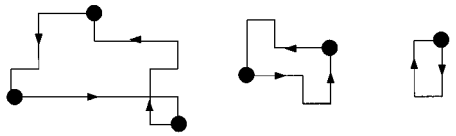

FIG. 1. A schematic configuration for six bosons after projecting the imaginary-time paths onto the xy plane. There are a total of three cycles: one cycle of one particle, one cycle of two particles, and one cycle of three particles. Solid circles denote particle positions at $\tau = 0$ and β.

a boson-only effective theory which we study numerically in this work. The system is described by the partition function $Z = \int \mathcal{D}\mathbf{x} e^{-S_{\text{eff}}}$ where the effective action is given by

$$S_{\text{eff}} = S_B^0 + S_2 \quad (15)$$

with

$$S_2 = \frac{1}{2}\sum_{\alpha\alpha'} \int_0^\beta \int_0^\beta \tilde{D}(\mathbf{x}_\alpha(\tau) - \mathbf{x}_{\alpha'}(\tau'))\dot{\mathbf{x}}_\alpha\cdot\dot{\mathbf{x}}_{\alpha'} d\tau d\tau', \quad (16)$$

where $\tilde{D}(\mathbf{x}) = (1/\beta L^2)\Sigma_{\mathbf{k}\neq 0} D(\mathbf{k},0) e^{-i\mathbf{k}\cdot\mathbf{x}}$. Note that the $\mathbf{k} = 0$ contribution has been excluded in the sum over $\mathbf{k}$, corresponding to a gauge choice where the $\mathbf{k} = 0$ part of $\mathbf{a}$ is zero. This is one way to fix the remaining degree of gauge freedom which is not determined by the condition of $\nabla\cdot\mathbf{a} = 0$. If we consider a system with periodic boundary conditions in space, another scheme would be to fix the line integral of the gauge field around a specified path which wraps around the boundary. However, the latter scheme is inconvenient for our purposes because it breaks translational invariance explicitly.

The current interaction $D(\mathbf{x})$ mediated by the gauge field is logarithmic at large distances, and is attractive between opposite currents. Due to the quasistatic nature of the gauge fields, the interaction is also infinitely retarded in time. We will see in the next section that this encourages world lines to retrace themselves, with important consequences for the boson dynamics.

Before proceeding to discuss the physical consequences of the current interaction S_2, some remarks about our averaging procedure for the gauge fields are in order. We have performed an ''annealed'' average over the gauge fields, rather than a ''quenched'' average. Annealed averaging is necessary in our case because our gauge field $\mathbf{a}$ is an internal thermodynamic variable. Formally, we evaluate observables $\langle\mathcal{O}\rangle$ as:

$$\frac{1}{Z}\int \mathcal{D}\mathbf{x}\mathcal{O}e^{-S_{\text{eff}}} = \frac{\int \mathcal{D}\mathbf{x}\mathcal{D}\mathbf{a}P[\mathbf{a}]\mathcal{O}e^{-S_B^0 - i\int\mathbf{a}\cdot d\mathbf{x}}}{\int \mathcal{D}\mathbf{x}\mathcal{D}\mathbf{a}P[\mathbf{a}]e^{-S_B^0 - i\int\mathbf{a}\cdot d\mathbf{x}}}, \quad (17)$$

where $P[\mathbf{a}] = \mathcal{N}^{-1}\delta(\nabla\cdot\mathbf{a})e^{-S_G[\mathbf{a}]}$ is the probability distribution for the gauge field, and $\mathcal{N}$ is a suitable normalization factor. This is different from quenched averaging, which would be appropriate if we dealt with a system with frozen impurities, such as a vortex glass. Quenched averaging requires the evaluation of

$$\int \mathcal{D}\mathbf{a}P[\mathbf{a}]\left[\frac{\int \mathcal{D}\mathbf{x}\mathcal{O}e^{-S_B^0-i\int \mathbf{a}\cdot d\mathbf{x}}}{\int \mathcal{D}\mathbf{x}e^{-S_B^0-i\int \mathbf{a}\cdot d\mathbf{x}}}\right]. \tag{18}$$

The differences between quenched and annealed averaging from the point of view of perturbation (diagrammatic) theory has been addressed elsewhere.[17,24]

From the point of view of the path-integral Monte Carlo method, our ability to perform the annealed averaging means that we would not have to perform extensive averages over different frozen realizations of the random flux. Moreover, note that the effective action (15) is manifestly real, and so we avoid the sign problem which occurs numerically when performing a quenched average over the gauge fields. We have studied boson densities between $n_b=1/4$ and 1/6. We choose an on-site interaction strength $U\geqslant 4t$. We follow the Monte Carlo methods of Ceperley and Pollock[25] and Trivedi.[26] Each Monte Carlo step involves the reconstruction of the world lines, $\{\mathbf{x}_\alpha(\tau)\}$, for all N particles using the ideal boson propagator in a short interval in imaginary time. The on-site interaction and the current interaction S_2 are taken into account using Metropolis tests. To ensure quantum exchange, we may insist that each accepted configuration differs from the previous one by a pair exchange. This can be incorporated, without loss of detailed balance, as a Metropolis test. We refer readers to the original references[25,26] for further details. (In evaluating the gauge field contribution S_2, we have also made use of a geometrical interpretation of S_2 which we discuss in the next section.) In the discretization of the imaginary time, we have used a small $\Delta\tau=\beta/M\leqslant 0.1/t$, so as to minimize the systematic error and to allow the reliable use of maximum entropy techniques to perform analytic continuation on our imaginary-time data to obtain the dynamical quantities of interest. This sets the lowest accessible temperature to $T\sim 0.1t$ for lattice sizes considered here. For studies on dynamic response to be discussed below, we have restricted ourselves to lattices of sizes up to 6×6, due to the need to obtain imaginary-time correlation functions to a high accuracy. For the calculation of static properties, we have studied lattices as large as 10×10.

To summarize, we have obtained an effective theory of bosons with current interactions which are long-ranged in space and time. This model can be studied using path-integral Monte Carlo methods. In the next section, we will discuss how these interactions affect the geometry of the boson world lines and hence the physical properties of the system.

IV. EFFECT OF GAUGE FIELDS ON WORLD-LINE GEOMETRY

A. ''Brinkman-Rice bosons''

In this section, we will discuss how the current interaction S_2 mediated by the gauge field affects world-line geometry. On the infinite plane, there is a simple geometrical interpretation of this interaction in terms of the winding numbers of the boson world lines. The winding number $w_{\mathbf{r}}$ around a plaquette $\mathbf{r}$ is the number of times the imaginary-time world lines of all the bosons wind around the plaquette. Consider the partition function before averaging over the gauge field. The effect of the gauge field enters the partition function as the phase factor $\exp[-i\Sigma_\alpha\int \mathbf{a}\cdot d\mathbf{x}_\alpha]$ in Eq. (12) over the gauge field. This phase factor can be written in terms of $w_{\mathbf{r}}$: $\Sigma_\alpha\int \mathbf{a}\cdot d\mathbf{x}_\alpha=\Sigma_{\mathbf{r}}w_{\mathbf{r}}\Phi_{\mathbf{r}}$. We can now perform the average directly over the Gaussian flux distribution (10), instead of the gauge-field distribution (9). We will be working with periodic boundary conditions (i.e., on a torus). This will be well-defined if we impose a constraint of zero total flux through the system. On averaging, the phase factor becomes

$$\begin{aligned}
&\int d\lambda \int \prod_{\mathbf{r}} d\Phi_{\mathbf{r}} \exp\left(-\sum_{\mathbf{r}} \frac{\Phi_{\mathbf{r}}^2}{2\langle\Phi^2\rangle} - \frac{2\pi i}{\Phi_0} \right. \\
&\left. \times \sum_{\mathbf{r}} w_{\mathbf{r}}\Phi_{\mathbf{r}} + i\lambda \sum_{\mathbf{r}} \Phi_{\mathbf{r}} \right) \\
&\propto \int d\lambda \exp\left(-2\pi^2 \frac{\langle\Phi^2\rangle}{\Phi_0^2} \sum_{\mathbf{r}} (w_{\mathbf{r}}+\lambda)^2 \right) \\
&\propto e^{-S_2},
\end{aligned}$$

$$S_2 = 2\pi^2 \frac{\langle\Phi^2\rangle}{\Phi_0^2}\left[\sum_{\mathbf{r}} w_{\mathbf{r}}^2 - \frac{1}{L^2}\left(\sum_{\mathbf{r}} w_{\mathbf{r}} \right)^2 \right]. \tag{19}$$

Thus we see that the action cost due to the current interaction is proportional to a geometrical property of the world lines, similar to an unoriented area, which has been termed the ''Amperean area'':[15]

$$\mathcal{A}_a = \left[\sum_{\mathbf{r}} w_{\mathbf{r}}^2 - \frac{1}{L^2}\left(\sum_{\mathbf{r}} w_{\mathbf{r}} \right)^2 \right]. \tag{20}$$

This geometrical interpretation of S_2 is particularly useful in the numerical evaluation of this quantity.

If we are working with periodic boundary conditions, the geometrical definition of $w_{\mathbf{r}}$ given above will not work because there is an ambiguity in identifying which plaquettes are inside or outside a loop on a torus. Nevertheless, we can still use the above analysis for paths which do not wrap around the boundaries. (We will discuss wrapping paths in the next section.) The only modification is that we need a definition of the winding numbers which preserves Stokes' theorem: $\oint \mathbf{a}(\mathbf{x})\cdot d\mathbf{x}=\Sigma_{\mathbf{r}}w_{\mathbf{r}}\Phi_{\mathbf{r}}$. In the case of zero total flux, a suitable definition is $w_{\mathbf{r}}=\tilde{\Phi}^{-1}\oint[\mathbf{a}_{\mathbf{r}}^0(\mathbf{x})-\mathbf{a}_{\mathbf{R}}^0(\mathbf{x})]\cdot d\mathbf{x}$, where $\mathbf{a}_{\mathbf{r}}^0(\mathbf{x})$ is the vector potential at $\mathbf{x}$ due to a test flux $\tilde{\Phi}$ placed at plaquette $\mathbf{r}$, and $\mathbf{R}$ is an arbitrary reference plaquette. Geometrically, this picks $\mathbf{R}$ to be on the ''outside'' of any loop on the torus. The Amperean area as defined above is independent of the choice of this plaquette, because different choices amount to global changes in the winding numbers (e.g., $w_{\mathbf{r}}\rightarrow w_{\mathbf{r}}+1$) and the above definition is invariant under such changes.

The effect of the gauge field on the particles is now clear. The action S_2 suppresses world-line loops with large winding numbers. Indeed, since S_2 is non-negative, it excludes all configurations with finite Amperean area in the limit of infinite $\langle\Phi^2\rangle$. This suppression can be related to the original problem of holes moving in a spin liquid with a slowly varying spin quantization axis. A hole moving in a loop comes back with a random phase due to the locally fluctuating spin chiralities of the spin background.[13] The random phase can be interpreted as arising from a fictitious random flux.

World-line loops that enclose large areas are strongly suppressed when averaged over random flux distribution due to the destructive interference of the random phases. Therefore, we expect that, in the presence of strong random flux, the dominant contribution to the partition function comes from a special kind of paths that do not ''see'' the random flux, i.e., paths where $\int \mathbf{a}\cdot d\mathbf{x}=0$. These are ''retracing paths'' where each traversal of a link on the lattice is retraced in the opposite direction at some point in time,[27,28] and such paths have zero Amperean area.

A similar picture of retracing paths has been studied by Brinkman and Rice,[27] who studied a single hole in a Mott insulator where the spins are treated classically. Indeed, studies of a single particle in a strong random flux have yielded a density of states nearly identical to that of the Brinkman-Rice problem.[29–31] The Brinkman-Rice model gives a linear-T resistivity at high temperatures ($T>t$) but a constant scattering rate of order t. Although we might expect this to be applicable to our model far above the degeneracy temperature of the bosons, this behavior does not extend down to the degenerate regime relevant to the present problem.

At boson densities of interest here and at low temperatures, Bose statistics and particle exchange are important; they can give rise to behavior different from the single-particle Brinkman-Rice result. We shall look at the effect of the gauge field on the quantum exchanges among bosons more carefully in Sec. IV C. For now, we point out that, even in the presence of strong gauge-field fluctuations, the bosonic nature of the particles cannot be ignored because the particles can form long exchange cycles that retrace themselves so that an individual boson does not have to retrace its own path. This is an important consideration at low temperatures where the imaginary-time paths are long, allowing for a strong degree of particle exchange. Although the system can be highly degenerate at low temperatures, we shall now argue that these ''Brinkman-Rice bosons'' remain normal at all finite temperatures, due to interactions with the fluctuating gauge fields.

B. Destruction of superfluidity

We will now discuss the effect of the gauge-field fluctuations on the superfluidity of the Bose system. We will see, as in the previous section, that this can be understood in terms of the geometrical properties of the boson world lines.

A neutral Bose system with short-range interaction in two dimensions is a superfluid below Kosterlitz-Thouless temperature T_{KT}. The onset of superfluidity at T_{KT} is caused by the binding of vortex-antivortex pairs in the Bose fluid so that vortex motion does not cause phase slips across the system. An essential ingredient of the existence of the superfluid phase is a long-range logarithmic attraction between the vortices and the antivortices. A single vortex costs infinite energy in an infinite system $E_v=(\pi\rho_s/m)\ln(L/a)$ where a is a short distance cutoff ($\sim$ vortex core radius) and ρ_s is the superfluid density. Therefore single vortices cannot exist at low temperatures. Nevertheless, the proliferation of free vortices is possible above T_{KT} because this provides a gain in entropy which also scales as $\ln L$. However, in a charged Bose system, screening currents causes the vortex interaction to be short-ranged. In our problem, the vortex interaction becomes exponentially weak at distances beyond $\lambda_P=[T/2\rho_s t\langle\Phi^2\rangle]^{1/2}\Phi_0$, which can be interpreted as a penetration depth of the Bose fluid. Now, the creation of a single vortex costs a finite amount of energy[32,33] $E_v=(\pi\rho_s/m)\ln(\lambda_P/a)$. This no longer compensates the entropic gain from vortex-antivortex unbinding, and so we do not expect to see a sharp phase transition of the Kosterlitz-Thouless type at finite temperatures.

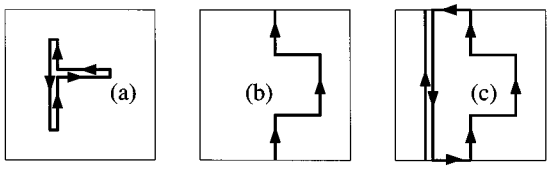

FIG. 2. (a) Projection of a world line onto the xy plane shows a retracing path. (b) A wrapping path. (c) Decomposition of (b) into a reference path and a nonwrapping path.

One might still expect that there is a crossover temperature scale below which the vortex density will be sufficiently low that the Bose system would have strong diamagnetic response. A rough estimate of this temperature scale using a Boltzmann weight for the vortex density gives a large value for this crossover temperature.[33] However, we will see later that, in the presence of strong gauge fluctuations, the diamagnetic response of the bosons remains small.

To understand the suppression of superfluidity specifically in our model, we turn to the path-integral formulation of the problem with periodic boundary conditions (i.e., on a torus). Ceperley and Pollock[25] have shown that superfluidity is associated with the existence of long world-line cycles which wrap around the torus. The superfluid density is given by

$$n_s=\frac{\langle \mathbf{W}^2\rangle}{4\beta t}, \tag{21}$$

where W_x (W_y) is the number of times the boson world lines wrap around the torus in the x (y) direction. In other words, $\mathbf{W}=\sum_{\alpha=1}^{N}\int_0^\beta d\tau \dot{\mathbf{x}}_\alpha/L$. In the presence of gauge fields, superfluidity is destroyed by the same mechanism that causes the Brinkman-Rice behavior: wrapping configurations pick up random phases, and should be suppressed by destructive interference on averaging over the gauge field. The number of plaquettes whose random fluxes contribute to the phase picked up by a wrapping path should increase with increasing system size. For a large enough system, one might expect this phase to be totally random. We therefore expect this suppression to be very strong. For instance, one can evaluate S_2 for a straight-line path which wraps around the torus in the y direction. To do so, we use Eq. (16) instead of Eq. (19) because the geometrical interpretation of S_2 in terms of winding numbers is not applicable for wrapping paths. We find that such a path gives

$$S_2=\frac{W_y^2}{2\beta}\sum_{k_x\neq 0,\ k_y=0} D(\mathbf{k},0)\simeq 2\pi^2 W_y^2 L^2\frac{\langle\Phi^2\rangle}{\Phi_0^2}. \tag{22}$$

To compute S_2 for a more general path with wrapping W_y, one can break it down into a wrapping path with the same wrapping number and a nonwrapping path (Fig. 2). (S_2 will

consist of the contributions of the wrapping paths and non-wrapping paths separately, as well as a cross term between the two paths.) We argue that S_2 diverges for all wrapping paths in the thermodynamic limit, and so superfluidity is destroyed at all finite temperatures.

It should be noted that we are studying a gauge model where the uniform part of **a** is set to zero. We may alternatively work with a model without this gauge fixing. With periodic boundary conditions, this model allows an arbitrary Aharonov-Bohm (AB) flux through the torus. This flux is related to the phase of the product of RVB parameters (ξ_{ij}) along a (Wilson) loop which wraps around the torus. If we average over this AB flux assuming a uniform distribution, we would find that all wrapping paths are strictly prohibited and $n_s=0$ at *all* temperatures even for samples of finite size. We will not impose such a drastic condition on the wrapping paths in this work.

We can also ask whether long-range order exists in the Green's function for the bosons. The Green's function itself $\langle b^\dagger(\mathbf{r})b(0)\rangle$ is not gauge invariant, and would vanish on averaging over different gauges. However, we can study the Green's function in a fixed gauge, for example, the transverse gauge $\nabla\cdot\mathbf{a}=0$. In fact, one can write a gauge-invariant analogue correlation function which coincides with the Green's function in the transverse gauge:[34]

$$G(\mathbf{r})=\langle b^\dagger(\mathbf{r})b(0)\rangle_{\nabla\cdot\mathbf{a}=0}$$
$$=\left\langle b^\dagger(\mathbf{r})b(0)\exp\left(-i\int d^2\mathbf{r}'f(\mathbf{r}')\nabla\cdot\mathbf{a}(\mathbf{r}')\right)\right\rangle, \tag{23}$$

where $\nabla^2_{\mathbf{r}'}f(\mathbf{r}')=\delta(\mathbf{r}'-\mathbf{r})-\delta(\mathbf{r}')$. In the path-integral representation, the evaluation of G involves a world line originating at site **r** and a world line terminating at site 0 at the same point in imaginary time. Note that this quantity coincides with the Green's function in the Coulomb gauge. Consider now the phase factor $\Sigma_\alpha\int\mathbf{a}\cdot d\mathbf{x}_\alpha$ picked up by the world lines $\{\mathbf{x}_\alpha\}$ in the evaluation of the Green's function $G(\mathbf{r})$ in this gauge. The random flux $\Phi_{\mathbf{R}}$ at a distant plaquette **R** (with $R\gg r$) has a contribution of magnitude $\Phi_{\mathbf{R}}/R$ to the vector potential at a point Q near 0 and **r**. The sum of the contributions to the vector potential at Q due to the random fluxes at radius R from the origin is a random vector with a mean squared magnitude of $2\pi R\times(\langle\Phi^2\rangle/R^2)\sim\langle\Phi^2\rangle/R$. This analysis is valid for all fluxes which are at a distance $R>r$. Integrating over the contribution of such fluxes, the variance of the magnitude of the vector potential at Q scales as $\langle\Phi^2\rangle\ln(L/r)$. Summing over all Q near 0 and **r**, we obtain a random phase with a divergent variance: $\langle\Phi^2\rangle r^2\ln(L/r)$. Thus, averaging over the distant fluxes for these sites, one obtains a suppression factor of $\exp[-\langle\Phi^2\rangle r^2 g(r/L)]$ where $g(x)\sim\ln 1/x$ for small x. This can be interpreted as a binding potential for the end points of $G(\mathbf{r})$. We therefore do not find long-range order in this quantity because of the destructive interference of the random phases due to distant fluxes. We will now present numerical evidence for the suppression of superfluidity below the degeneracy temperature T_{D0} of the system. A measure of the degeneracy temperature is the Kosterlitz-Thouless temperature of the system at zero flux. We make use of the observation of Ceperley and Pollock[35]

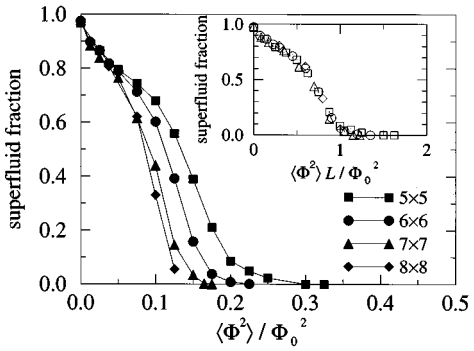

FIG. 3. Superfluid density vs $\langle\Phi^2\rangle$ for different system sizes at $\beta t=6$. Inset: a scaling plot suggests that superfluidity vanishes at $\langle\Phi^2\rangle_c\sim 1/L$.

that the the probability of bosons to participate in the multiparticle exchange is about $\frac{1}{2}$ at the Kosterlitz-Thouless transition. In other words, the probability P_1 that a boson is in an exchange cycle of length 1 is about $\frac{1}{2}$. We estimate that, for our lattice bosons with density $n_b=0.25$ and on-site interaction $U=4t$, the degeneracy temperature $T_{D0}=1.1t$. (For strong on-site repulsion, T_{D0} is not particularly sensitive to the value of U, e.g., $T_{D0}=0.9t$ for $U=16t$.)

We have measured, using Eq. (21), the superfluid fraction n_s/n_b at $T=t/6$ with $U=4t$ for a range of flux variances and for systems up to 8×8 in size (Fig. 3). We see that the superfluid fraction decreases with increasing system size. In fact, the superfluid fraction as a function of $\langle\Phi^2\rangle L$ collapses onto a single curve (Fig. 3, inset), indicating that $n_s(L,\beta,\langle\Phi^2\rangle)=f(L\langle\Phi^2\rangle,\beta)$. Since $f(x,\beta)\to 0$ as $x\to\infty$, we see that an arbitrarily small random magnetic flux would destroy superfluidity in the thermodynamic limit. In the language of the renormalization group, this shows that the scattering by gauge fields is a relevant perturbation at finite temperature.

C. World-line geometry in the normal phase

Having established that our system remains normal at low temperatures, we will now examine the geometry of the world lines in this normal phase in the presence of strong gauge fluctuations. In particular, we will look at the effect of the gauge fields on quantum exchange and imaginary-time diffusion. These are mutually related: imaginary-time diffusion over large distances aids quantum exchange among particles and quantum exchange facilitates imaginary-time diffusion. For example, in a dissipative model of bosons coupled to an external heat bath, a slow logarithmic imaginary-time diffusion is expected to suppress quantum exchange very strongly, resulting in an incoherent liquid even at zero temperature.[14,36] In our case, the bosons are elastically scattered by the gauge fields. We find that the gauge fields have a less dramatic effects on quantum exchange and imaginary-time diffusion.

We have shown that the world lines retrace themselves in the presence of random flux. One might expect that, compared with the case of zero flux, this would reduce the distance traveled by the particles in the imaginary-time interval β before their paths must return to some permutation of their starting positions. This should slow down the imaginary-time

TABLE I. One-, two-, three-, and four-boson exchange probability for various T, $\langle\Phi^2\rangle$, and U at quarter-filling.

T	U	$\langle\Phi^2\rangle/\Phi_0^2$	P_1	P_2	P_3	P_4
$0.5t$	$4t$	0.5	0.51	0.23	0.13	0.07
$0.5t$	$4t$	0	0.20	0.12	0.11	0.11
$0.25t$	$4t$	0	0.12	0.11	0.11	0.11
$0.25t$	$4t$	0.5	0.26	0.16	0.13	0.12
$0.25t$	$16t$	0.5	0.41	0.21	0.13	0.10
$0.11t$	$4t$	0	0.11	0.11	0.11	0.11
$0.11t$	$4t$	0.5	0.12	0.11	0.11	0.11
$0.11t$	$16t$	0.5	0.12	0.11	0.11	0.11

motion of the bosons as well as reduce the probabilities for exchange. We find that this is indeed the case.

We first look at the exchange probabilities P_i of a particle participating in an exchange cycle of i bosons. As before, we may deduce a degeneracy temperature T_D from the probability $(1-P_1)$ for a particle to be involved in particle exchange.[37] This degeneracy temperature is reduced compared to the case of zero flux. For $U=4t$ at quarter filling, we find that the zero-flux degeneracy temperature $T_{D0}=1.1t$ is reduced to $T_D=0.5t$ at $\langle\Phi^2\rangle=0.5\Phi_0^2$. At $\frac{1}{6}$-filling, it is reduced from $T_{D0}=0.8t$ to $T_D=0.34t$. A finite T_D does not imply Bose condensation at a finite temperature. Indeed, one cannot deduce a superfluid transition by examining the exchange probabilities. Remarkably, in the degenerate regime below T_D, the exchange probabilities for the cases of $\langle\Phi^2\rangle=0$ and $0.5\Phi_0^2$ are nearly identical (see Table I). In this temperature regime, a particle is equally likely to participate in an exchange cycle of any size: $P_1\simeq P_2\simeq\cdots\simeq P_N\simeq 1/N$.

We can gain a qualitative understanding of the low-temperature exchange probabilities by examining how the suppression of Amperean area by S_2 affects the geometry of the world-line configurations. When there is significant quantum exchange, individual bosons do not have to retrace their own paths in order to minimize the total Amperean area of the world-line configuration of all the bosons. Instead, one might minimize the Amperean area of each world-line loop formed by several bosons in the same exchange cycle. We find that this is not the entire situation at sufficiently low temperatures. Below T_D, the different world-line loops have strong overlap. We find that different cycles retrace each others' paths (see Fig. 4). Thus, although the gauge fields have a drastic effect on the *total* area enclosed by all the boson world lines, individual world-line cycles may enclose large areas. One might therefore expect that aspects of the world-line geometry, which are insensitive to the total area, may be very similar to the case of zero flux.

The observation that individual particles do not have to retrace their own paths suggests that they could diffuse a greater distance than in the single-particle case. One should see a reduction in the kinetic energy $\langle K\rangle$ of the particles compared to the Brinkman-Rice theory.[27] This is indeed the case. (See the Appendix for a discussion of the measurement of the kinetic energy.) A single particle with retracing paths has a band edge at $-2\sqrt{3}t$ rather than $-4t$. In our system,

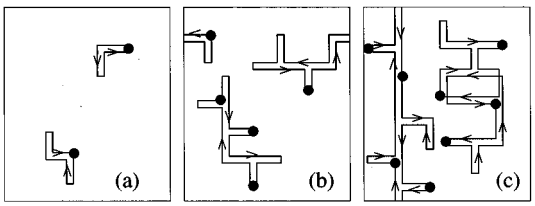

FIG. 4. Schematic world-line cycles which retrace when projected onto the xy plane. Solid circles denote boson positions at $\tau=0$. (a) Each boson retraces its own path; (b) exchange cycles with more than one boson retrace their own paths; (c) two exchange cycles can retrace each others' paths, and two wrapping paths can retrace each other to give zero total wrapping around the boundaries.

the kinetic energy per particle goes below the Brinkman-Rice band edge at low temperatures, approaching $-4t$ roughly linearly in temperature (Fig. 5). Thus, we see that the strong gauge fluctuations do not have a large effect on some aspects of the world-line geometry (e.g., exchange probabilities) while having a dramatic influence on others (e.g., superfluidity).

Let us now examine the imaginary-time motion of the particles in more detail. Ideal bosons are diffusive in imaginary time at all temperatures, i.e., the mean-squared displacement of particle α is linear in imaginary time τ: $R^2(\tau)=\langle[\mathbf{x}_\alpha(\tau)-\mathbf{x}_\alpha(0)]^2\rangle=4t\tau$ for $0<\tau<\beta/2$. With repulsive interactions, there is an increase in the effective mass of the particle, e.g., for $U=4t$ at quarter filling, we find $t\rightarrow t^*=0.95t$. In the presence of random magnetic flux, the imaginary-time diffusion is slowed down, and the mean-squared displacement $R^2(\tau)$ is no longer linear in τ at all temperatures. Figure 6 shows our results for the (superfluid) zero-flux case at temperature $\beta t=9$ and the case of strong random flux at $\beta t=4,6,9$. Since we are working with periodic boundary conditions, we have used the definition: $R^2(\tau)=\langle[\int_0^{\beta/2}\dot{\mathbf{x}}_\alpha(\tau)d\tau]^2\rangle$. We can see that, whereas $R^2(\tau)$ has significant downward curvature at $\beta t=2$, it becomes closer to diffusive behavior as the temperature is lowered. However, we are unable to reach the asymptotic regime where the particle has traveled far on the scale of the interparticle spacing over a time period of $\beta/2$ (see Fig. 6 inset).

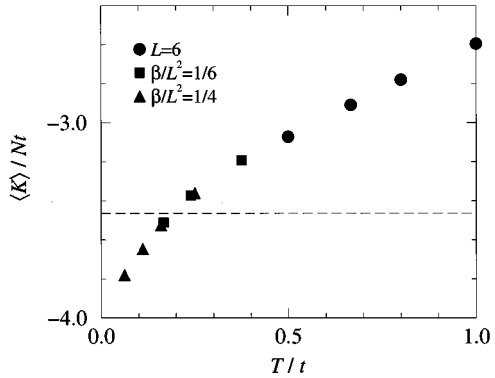

FIG. 5. Kinetic energy per particle as a function of temperature. Dashed line marks the Brinkman-Rice band edge for the single-particle problem. $\langle\Phi^2\rangle=0.5\Phi_0^2$ and $U=4t$.

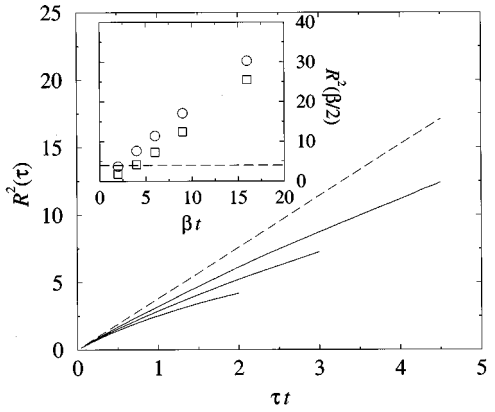

FIG. 6. Single-particle diffusion $R^2(\tau)=\langle[\mathbf{x}(\tau)-\mathbf{x}(0)]^2\rangle$ in imaginary time for $0<\tau<\beta/2$. Solid lines: strong random flux with $\langle\Phi^2\rangle=0.5\Phi_0^2$ at $\beta t=4,6,9$. Dashed line: zero flux at $\beta t=9$. Inset: $R^2(\beta/2)$ for zero flux (○) and $\langle\Phi^2\rangle=0.5\Phi_0^2$ (□); dashed line marks the squared interparticle spacing.

In order to study the long-time behavior, we can examine the size of the world-line exchange cycles. A cycle where the world lines of l particles $\{\mathbf{x}_1,\ldots,\mathbf{x}_l\}$ form a loop can be roughly regarded as a particle traveling over a time interval of $l\beta$. Exchange allows such a world-line cycle to cover large distances compared with an individual boson. In a system with periodic boundaries, the size R_l of the cycle is defined by:

$$R_l^2=\left\langle\left[\int_0^{\beta/2}\dot{\mathbf{x}}_{(l+1)/2}d\tau+\sum_{\alpha=1}^{(l-1)/2}\int_0^{\beta}\dot{\mathbf{x}}_\alpha d\tau\right]^2\right\rangle,\quad l\ \text{odd}$$
$$=\left\langle\left[\sum_{\alpha=1}^{l/2}\int_0^{\beta}\dot{\mathbf{x}}_\alpha d\tau\right]^2\right\rangle,\quad l\ \text{even}. \tag{24}$$

For ideal bosons, R_l^2 should equal $R^2(\tau=l\beta/2)$ at inverse temperature $l\beta$, and therefore should scale linearly with l. Figure 7 shows R_l^2 for a 4×4 lattice with nine particles. We have measured only cycles which do not have a net wrapping number around the periodic boundaries so that we do not have contributions from cycles with different topologies. We see that R_l^2 is linear in l for the cases of zero flux and strong random flux, although the slope of the case with the strong random flux is reduced substantially. This demonstrates that the imaginary-time motion of the bosons is diffusive at long distances.

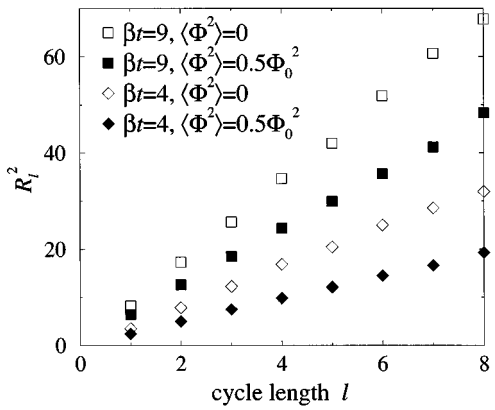

FIG. 7. Cycle sizes R_l^2 as a function of cycle length l for a 6×6 lattice with nine particles.

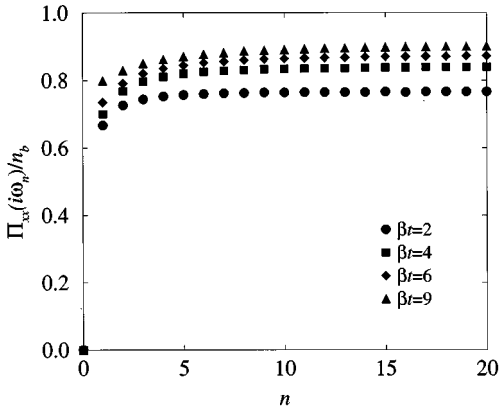

FIG. 8. Current correlation function $\Pi_{xx}(i\omega_n)$ for a 6×6 lattice with nine bosons with $\langle\Phi^2\rangle=0.5\Phi_0^2$ and $U=4t$.

These results indicate that we are probing an unconventional phase of a Bose liquid. Although the system remains normal, many aspects of the imaginary-time motion of the particles in the degenerate regime resemble that of a neutral Bose liquid which is a superfluid in such temperatures. In subsequent sections, we shall study the physical properties of this ''strange metal'' and discuss the relevance to the normal state of the cuprate superconductors.

V. TRANSPORT AND OPTICAL CONDUCTIVITY

In this section, we will present our quantum Monte Carlo (QMC) results on longitudinal transport for this strange Bose metal. To obtain the conductivity of the system, we measure its imaginary-time analogue $\sigma_{\alpha\beta}(i\omega_n)$ in our quantum Monte Carlo simulation:

$$\sigma_{\alpha\beta}(i\omega_n)=\frac{1}{|\omega_n|}\Pi_{\alpha\beta}(i\omega_n), \tag{25}$$

$$\Pi_{\alpha\beta}(i\omega_n)=\int_0^{\beta}\langle j^{\alpha}_{\mathbf{q}=0}(\tau)j^{\beta}_{\mathbf{q}=0}(0)\rangle e^{i\omega_n\tau}d\tau, \tag{26}$$

where $\mathbf{j}_\mathbf{q}(\tau)=\Sigma_\mathbf{r}\mathbf{j}_\mathbf{r}(\tau)e^{i\mathbf{q}\cdot\mathbf{r}}$ and $\mathbf{j}_\mathbf{r}(\tau)=\Sigma_\alpha\delta(\mathbf{r}-\mathbf{x}_\alpha(\tau))(d\mathbf{x}_\alpha/d\tau)$ is the gauge-invariant current (Fig. 8).

The imaginary-time measurements are related to the real-time conductivity $\sigma(\omega)\equiv\sigma_{xx}(\omega)$ by

$$-\frac{1}{2L^2}\langle\mathbf{j}_{\mathbf{q}=0}(\tau)\cdot\mathbf{j}_{\mathbf{q}=0}(0)\rangle=\int_{-\infty}^{\infty}\frac{\omega e^{-\omega\tau}\sigma(\omega)}{1-e^{-\beta\omega}}\frac{d\omega}{\pi}. \tag{27}$$

Deducing dynamical properties (such as conductivity) from imaginary-time data is in general an ill-posed problem. Several approximate methods are often used in the context of QMC studies. A simple method, which has been used in the study of the superfluid-insulator transition,[38,39] is to fit $\sigma(i\omega_n)$ to a simple functional form, such as the Drude form $\sigma(i\omega_n)=\sigma_0/(1+|\omega_n|\tau_{\rm tr})$. More generally, one can use a Padé approximant to fit an arbitrary number of poles and zeros:

$$\sigma(z)=\frac{a_0+a_1z+\cdots+a_{N_n}z^{N_n}}{b_0+b_1z+\cdots+b_{N_d}z^{N_d}}. \tag{28}$$

This approach is particularly suitable if the scattering rate $1/\tau_{\rm tr}$ [or the position of the pole closest to the origin in (28)] is large compared to the temperature at low temperatures. This is, however, not the case in our problem. In our system, $\Pi_{xx}(i\omega_n)$ is nearly constant as a function of n for finite n even at low temperatures, suggesting that $1/\tau_{\rm tr}$ is proportional to T. [Note that $\Pi_{xx}(n=0)=0$ in the limit of strong random flux because paths which wrap around the torus are strongly suppressed.]

We have calculated the conductivity by numerical analytic continuation using the maximum-entropy (MaxEnt) method.[40,41] Equation (27) takes the form of a linear integral equation:

$$d(\tau)=\int K(\tau,\omega)r(\omega)d\omega, \tag{29}$$

where $K(\tau,\omega)$ is the kernel relating the imaginary-time data $d(\tau)$ to the response function $r(\omega)$. In our QMC simulations, $d(\tau)$ is measured at discrete points $\tau_l=l\Delta\tau$ with mean $\bar{d}_l$. The errors for the time points l and m are correlated with a covariance matrix $C_{lm}=\overline{d_l d_m}-\bar{d}_l\bar{d}_m$. The MaxEnt method finds an estimate of $r(\omega)$ by optimizing the ''entropy'' S:

$$S=\int d\omega\left[r(\omega)-m(\omega)-r(\omega)\ln\frac{r(\omega)}{m(\omega)}\right], \tag{30}$$

defined relative to a default model $m(\omega)$, while ensuring a reasonable goodness of fit $\chi^2=\Sigma_{l,m}(D_l-\bar{d}_l)[C^{-1}]_{lm}(D_m-\bar{d}_m)$ where $D_l=\int d\omega K(\tau_l,\omega)r(\omega)$. This is achieved by maximizing the functional: $\phi[r(\omega);\alpha]=-\chi^2/2+\alpha S$. The variable α controls the tradeoff between the smoothness and the goodness of the fit, and ϕ is also maximized with respect to it.[42] We have chosen $m(\omega)$ to be a constant in order not to build in any bias. Our results are not sensitive to this choice. Details of the MaxEnt method are given in Refs. 40–42.

One can check the results of the MaxEnt inversion using relevant sum rules. In the case of conductivity, we have used the sum rule

$$\int_0^\infty \sigma(\omega)d\omega=-\frac{\pi}{4}\frac{\langle K\rangle}{L^2}, \tag{31}$$

which is the lattice version of the more familiar form in the continuum: $\int_0^\infty\sigma(\omega)d\omega=\pi n_b/2m$. In our MaxEnt results, this sum rule is obeyed to within 3% error. In order to obtain reliable data for the MaxEnt inversion, we have worked with a fine discretization in imaginary time ($t\Delta\tau\leqslant 0.1$). For the lowest temperatures ($T<0.4t$), we worked at fixed $\Delta\tau$ and β/L^2. We chose $\beta\propto L^2$ to control the finite-size effects because of the imaginary-time motion of the bosons is roughly diffusive, as discussed above. Our results are in fact not very sensitive to this choice, indicating that finite-size effects are small. For instance, the values of resistivity at $\beta t=4$ and $n_b=1/4$ for 4×4 and 6×6 are similar within statistical error.

We find that $\sigma(\omega)$ consists of a single Drude-like peak (Fig. 9). Since this peak exhausts the sum rule (31), its spectral weight is proportional to $-\langle K\rangle$. This spectral weight has a weak temperature dependence in this temperature range because, as already discussed, the kinetic energy approaches $-4t$ per particle as the temperature is lowered. This should be contrasted with the Brinkman-Rice result[27] for nondegenerate particles ($T\gg t$) where the weight under $\sigma(\omega)$ decreases as $\langle -K\rangle\sim T^{-1}$.

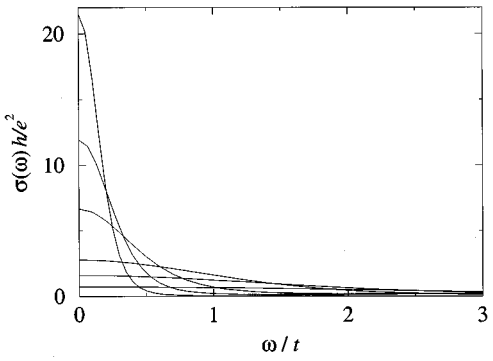

FIG. 9. Optical conductivity for 6×6 lattice with nine bosons at $\beta t=9,6,4,2,1,0.5$. $\langle\Phi^2\rangle=0.5\Phi_0^2$ and $U=4t$.

The width of $\sigma(\omega)$ gives a transport scattering rate consistent with: $1/\tau_{\rm tr}=\zeta k_B T$ with $\zeta=1.8-2.2$ (Fig. 10). This result has been obtained for two densities $n_b=1/4$ and 1/6 so that this scattering rate appears to be independent of density. Again this differs from the Brinkman-Rice result where $1/\tau_{\rm tr}$ is a constant of order t (as one begins to see at the highest T in Fig. 10). The resistivity ρ, given by the peak height, is consistent with a linear temperature dependence of $\rho e^2/h=(1/2\pi n_b)T/t$ for $T<2t$ (Fig. 11). We estimate a statistical error of 5% for ρ by examining fluctuations due to statistical errors in the measurement of the current correlation function. There are also systematic errors due to the smoothing of structures.

There appears to be a systematic deviation from the linear-T behavior below $T=0.3t$, in particular in the case of quarter filling. This deviation is stronger for ρ than for $1/\tau_{\rm tr}$. The difference can be attributed to the T dependence of the Drude weight discussed above which should affect the resistivity but not the relaxation time. We speculate that the deviation from linearity at the lowest temperatures may indicate the approach to zero-temperature critical behavior. This is beyond the scope of this paper.

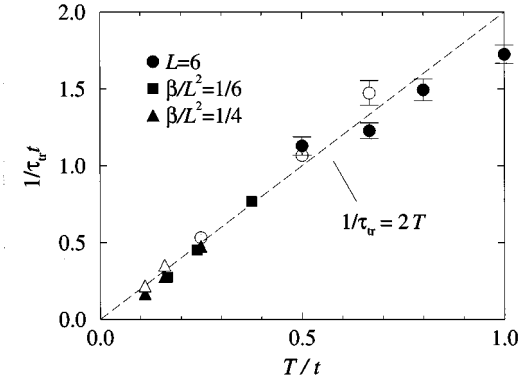

FIG. 10. Scattering rate $1/\tau_{\rm tr}$ as a function of temperature. Solid (hollow) symbols correspond to a boson density of $n_b=1/4$ (1/6). $\langle\Phi^2\rangle=0.5\Phi_0^2$ and $U=4t$.

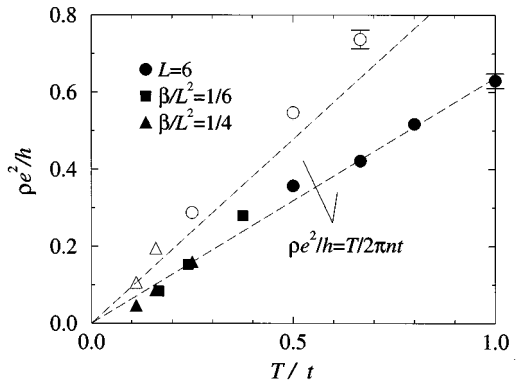

FIG. 11. Resistivity as a function of temperature. Solid (hollow) symbols correspond to a boson density of $n_b=1/4$ (1/6). $\langle\Phi^2\rangle=0.5\Phi_0^2$ and $U=4t$.

Our resistivity agrees, to within a factor of 2, with Jaklič and Prelovšek,[43] who provided an approximate diagonalization of the t-J model on 4×4 lattices and found a Drude peak with width $2T$. They also found a broad background, and interpreted it with a frequency-dependent scattering rate $\tau(\omega)$. Indeed, some authors have interpreted the experimental optical conductivity as possessing a power-law tail and emphasized its importance.[44] This incoherent part of the conductivity is absent from our boson model, and may be due to inelastic scattering of the bosons with the gauge field or, more generally, with the fermionic degrees of freedom.

VI. MAGNETIC RESPONSE

We now discuss the response of this degenerate Bose liquid to a weak external magnetic field perpendicular to the plane. In the absence of the random magnetic fields, a Bose liquid has a strong diamagnetic response as the temperature is lowered towards the transition to a superfluid when it develops a Meissner response. We argue here that the linear response of the system to a magnetic field is strongly suppressed by the gauge fluctuations. Qualitatively, this can be again understood by examining the world-line configurations. We have already demonstrated that the partition function is dominated by world-line paths which are unaffected by the internal gauge fields $\Sigma_\alpha\int\mathbf{a}\cdot d\mathbf{x}_\alpha=0$ for any $\mathbf{a}$. These configurations are therefore also unaffected by any external magnetic fields. Thus, we see that the system has a vanishing linear response to magnetic fields in the limit of strong gauge fluctuations. For the sake of completeness, we will now discuss more quantitatively the magnetic response of the system. Relevant physical quantities are the diamagnetic susceptibility χ_B, the Hall coefficient R_H, and the magnetoresistance $\Delta\rho/\rho$.

Consider first the diamagnetic susceptibility. On the infinite plane, in the presence of a weak external field H, each world-line configuration picks up an extra factor of $\exp[-i\Sigma_\alpha\mathbf{A}_{\rm ext}\cdot d\mathbf{x}_\alpha]=\exp[-iH\mathcal{A}_o]$ where curl$\mathbf{A}_{\rm ext}=H$, and $\mathcal{A}_o=\Sigma_{\mathbf{r}}w_{\mathbf{r}}$ is the oriented area of the configuration. (In this section, we will use units where $\Phi_0=2\pi$.) Expanding this in a Taylor series, one can write the partition function $Z(H)$ as

$$Z(H)=\int\mathcal{D}\{\mathbf{x}\}\left(1-iH\mathcal{A}_o-\frac{1}{2}H^2\mathcal{A}_o^2\right)e^{-S_{\rm eff}}$$

$$=Z(0)\left(1-\frac{1}{2}H^2\langle\mathcal{A}_o^2\rangle\right),\tag{32}$$

where $\mathcal{A}_o$ is the oriented area of a world-line configuration and $\langle\cdots\rangle$ denotes an average for the system at $H=0$. We have assumed here that the external magnetic field H has negligible effect on the spectrum of the gauge fluctuations. The diamagnetic susceptibility is given by

$$\chi_B=\frac{1}{\beta}\frac{\partial^2\ln Z}{\partial H^2}=\frac{4\pi^2T}{\Phi_0^2}\langle\mathcal{A}_o^2\rangle.\tag{33}$$

Since $\mathcal{A}_a>\mathcal{A}_o$ by definition, we can see that, when the gauge fluctuations are strong so that configurations with zero Amperean area dominate, the system has no diamagnetic response, as suggested in Sec. IV B.

It should be noted that, with periodic boundary conditions, the total flux penetrating the torus is quantized in units of the flux quantum. One should use replace $\langle\mathcal{A}_o^2\rangle$ by $4\langle\sin^2[H_0\mathcal{A}_o/2]\rangle/H_0^2$ where $H_0=\Phi_0/L^2$ is the smallest uniform field allowed in a torus of size L. Moreover, as in the case for the Amperean area, a geometrical interpretation of the phase factor $\int\mathbf{A}_{\rm ext}\cdot d\mathbf{x}$ is not possible for paths which wrap around periodic boundaries. However, these wrapping configurations are strongly suppressed in the case of strong random flux and should give negligible contribution to the susceptibility.

We can also consider magnetotransport properties. We need the current-current correlator at a small external field: $\langle j^\alpha(\tau)j^\beta(0)\rangle_H$. Expanding again in H and dropping terms which vanish by symmetry, one obtains

$$\langle j^\alpha j^\beta\rangle_H=\frac{\langle j^\alpha j^\beta\rangle-\frac{1}{2}H^2\langle j^\alpha j^\beta\mathcal{A}_o^2\rangle+\cdots}{1-\frac{1}{2}H^2\langle\mathcal{A}_o^2\rangle+\cdots}.\tag{34}$$

Using (26), we obtain the Hall conductivity σ_{xy}^H and the magnetoconductivity $\Delta\sigma_{xx}=\sigma_{xx}^H-\sigma_{xx}^{H=0}$:

$$\frac{\sigma_{xy}^H(i\omega_n)}{H}=\frac{2\pi i}{|\omega_n|\Phi_0}\int_0^\beta d\tau e^{i\omega_n\tau}\langle j^x_{\mathbf{q}=0}(\tau)j^y_{\mathbf{q}=0}(0)\mathcal{A}_o\rangle,$$

$$\frac{\Delta\sigma_{xx}(i\omega_n)}{H^2}=\frac{2\pi^2}{|\omega_n|\Phi_0^2}\int_0^\beta d\tau e^{i\omega_n\tau}[\langle j^x_{\mathbf{q}=0}(\tau)j^x_{\mathbf{q}=0}(0)\mathcal{A}_o^2\rangle$$

$$-\langle j^x_{\mathbf{q}=0}(\tau)j^x_{\mathbf{q}=0}(0)\rangle\langle\mathcal{A}_o^2\rangle].\tag{35}$$

Since the oriented area $\mathcal{A}_o$ can be written as $\mathcal{A}_o=\frac{1}{2}\Sigma_{\mathbf{r}}\int_0^\beta\hat{z}\cdot(\mathbf{j}_{\mathbf{r}}(\tau)\times\mathbf{r})d\tau$, we see that we can relate this expression for the Hall conductivity σ_{xy}^H to the more familiar one involving the average of three currents.[45] In principle, the quantities Im$\sigma_{xy}^H(\omega)$ (from which we can obtain Reσ_{xy}^H from a Kramers-Kronig relation) and $\Delta\sigma_{xx}(\omega)$ can be computed by analytic continuation. However, these quantities are too small to measure in the regime of strong gauge fluctuations that we study. Thus, we see that the magnetotransport response is strongly suppressed by the gauge fluctuations because it is sensitive to the oriented area of the world-line configurations.

Since we have argued that the gauge field fluctuations are indeed strong in the cuprates at temperatures above the superconducting transition, it appears that our simple boson model with a quasistatic gauge field cannot describe quantitatively the magnetotransport in these materials. This result is however qualitatively consistent with the experimental finding that these magnetotransport properties are generally suppressed from the classical values. To obtain a quantitative prediction for these properties, one may attempt to restore dynamics to the gauge fields. If the gauge field may relax in time, then the boson world lines no longer have to obey the condition of strictly retracing paths. This would allow the world lines to enclose a finite oriented area and hence a finite response to external magnetic fields. However, we emphasize that such an approach might not represent the physics completely. We believe that our model illustrates the general point that the influence of an external field on the system is strongly masked by the fluctuations of the internal magnetic field.

VII. DENSITY CORRELATION FUNCTION

A. Phase separation

Noninteracting bosons are infinitely compressible. They would therefore collapse into a small region of the system in the presence of any quenched disorder which has a tail of localized states in the single-particle spectrum. An analogous collapse is also found in this problem with annealed random flux. Such an instability was discussed by Feigelman *et al.*[33] who have argued that it occurs also in the case of interacting bosons at low densities, leading to a hole-rich phase and a hole-absent phase. They further argued a long-range Coulomb repulsion would be necessary to stabilize the uniform phase.

Within the world-line picture, one can visualize the instability of the homogeneous phase in the limit of strong gauge fluctuations. The condition of retracing paths in this limit encourages the bosons to come close to each other so that their paths may retrace each other. This will allow individual boson paths to explore a larger area (in imaginary time), and hence lower the kinetic energy of the system compared to the case with each boson has to retrace its own path. In the absence of any repulsive interactions, this effect would dominate at low temperatures, making the homogeneous phase unstable to collapse.

We find that this instability towards the formation of dense aggregates indeed occurs in our model in the absence of boson repulsion, although the instability is prevented by on-site repulsion, at least for the moderate boson densities of interest here. We have studied the instability by examining the compressibility of the system: $\kappa=\lim_{q\to 0}\kappa(\mathbf{q})$ with

$$\kappa(\mathbf{q})=\frac{1}{Nn_b}\int_0^\beta d\tau\langle n_{\mathbf{q}}(\tau)n_{-\mathbf{q}}(0)\rangle, \tag{36}$$

where $n_{\mathbf{q}}(\tau)$ is the Fourier transform of the boson density at imaginary time τ. Alternatively, $\kappa=\lim_{q\to 0}\beta S(\mathbf{q})/n_b^2$ where $S(\mathbf{q})$ is the static structure factor:

$$S(\mathbf{q})=\frac{1}{L^2}\langle n_{\mathbf{q}}(\tau)n_{-\mathbf{q}}(\tau)\rangle. \tag{37}$$

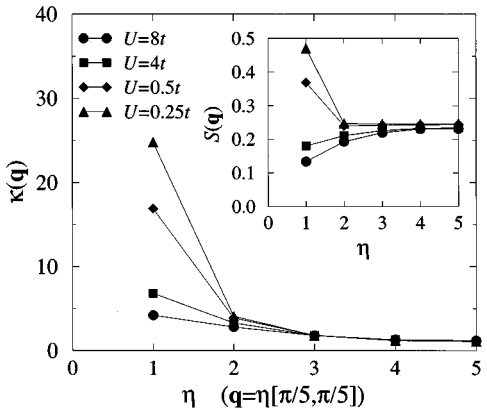

FIG. 12. Static structure factor (inset) and the **q**-dependent compressibility as a function of q in the (π,π) direction for different values of U. $\beta t=4$, $\langle\Phi^2\rangle=0.5\Phi_0^2$, $n_b=0.25$.

In Fig. 12, we show the behavior of $S(\mathbf{q})$ and $\kappa(\mathbf{q})$ for different values of the on-site repulsion U for a 10×10 lattice with 25 bosons. The structure factor $S(\mathbf{q})$ as a function of $\mathbf{q}$ is qualitatively different for the cases of small U and large U (compared to t): $S(\mathbf{q})$ for $\mathbf{q}=(\pi/5,\pi/5)$ is greater than the density n_b for when the on-site interaction is small. We can also look at the compressibility. Since we work with finite systems at fixed boson number, we will evaluate $\kappa(\mathbf{q})$ at the smallest wave vector of the system as an estimate of the $q=0$ behavior. We see that, in the presence of random magnetic flux, the compressibility increases with decreasing U. This can be interpreted as a divergence as $q\to 0$ for small U, and hence an instability of the homogeneous phase. [This is also reflected in the magnitude of the fluctuations in our QMC results for $\kappa(\mathbf{q})$ which grows as $q\to 0$ for sufficiently small U.] However, for strong on-site repulsion, the density correlations show no sign of an instability at this density.

B. Static structure factor

The density fluctuations in our boson model should be relevant to the charge fluctuations in the full t-J model. It has been pointed out that the density excitations of the t-J model does not resemble those of a conventional Fermi system. We will now compare our results with numerical results on the full t-J model in the literature.

The static structure factor (37) has been calculated by various means.[9,46] Figure 13 shows the static structure factor for our boson system together with that of the t-J model[9] at $T=0.25t$. We see that our results are qualitatively similar to the t-J model, with improving quantitative agreement as one approaches the hard-core limit (see, for example, $U=16t$). We should point out that this dependence on U should not be as strong for the transport properties of the system, because the particle currents are not directly affected by the repulsive density interactions.

It is also interesting to note that the magnitude of the gauge field fluctuations has a relative weak effect on $S(\mathbf{q})$ when the on-site repulsion U is strong. However, as we shall see in the next section, the *dynamics* of the density excitations is strongly modified by the interaction with the gauge fields.

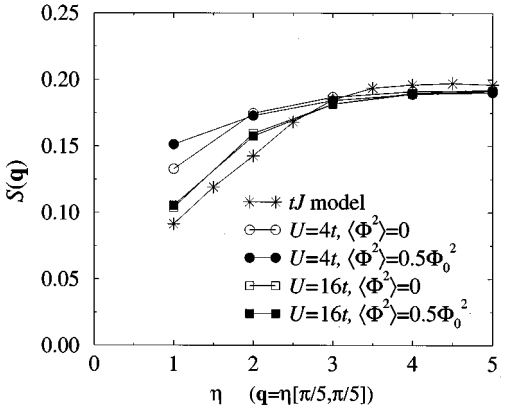

FIG. 13. Static structure factor of the boson model at density $n_b=0.2$ along the (π,π) direction at $T=0.25t$. Asterisks: t-J model result (Ref. 9) at electron density $n=1-n_b=0.8$ and $t/J=2$.

C. Dynamic structure factor

We discuss now the dynamic structure factor $S(\mathbf{q},\omega)$:

$$S(\mathbf{q},\omega)=\frac{1}{L^2}\int dt e^{i\omega t}\langle n_{\mathbf{q}}(t)n_{-\mathbf{q}}(0)\rangle, \tag{38}$$

where $n_{\mathbf{q}}(t)$ is the Fourier transform of the density in real time. The dynamic structure factor is related to the imaginary-time density-density correlation function by

$$\frac{1}{L^2}\langle n_{\mathbf{q}}(\tau)n_{-\mathbf{q}}(0)\rangle=\int_0^\infty (e^{-\tau\omega}+e^{-(\beta-\tau)\omega})S(\mathbf{q},\omega)d\omega. \tag{39}$$

Again, we use MaxEnt to perform the inversion of this integral equation. Two sum rules can be used as a check of the MaxEnt procedure:

$$\int_0^\infty d\omega(1-e^{-\beta\omega})\omega S(\mathbf{q},\omega)=-\frac{\langle K\rangle}{2L^2}(2-\cos q_x-\cos q_y)t,$$

$$\int_0^\infty d\omega\frac{1-e^{-\beta\omega}}{\omega}S(\mathbf{q},\omega)=\frac{1}{2}n_b^2\kappa(\mathbf{q}). \tag{40}$$

These are lattice versions of the f-sum rule and the compressiblity sum rule. They are satisfied within 1% error in our results.

Figure 14 shows $S(\mathbf{q},\omega)$ for our bosons with and without the random flux. The system in the absence of random flux

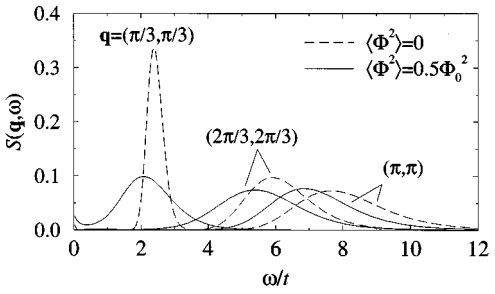

FIG. 14. Dynamic structure factor of the superfluid phase ($\langle\Phi^2\rangle=0$) and the normal phase ($\langle\Phi^2\rangle=0.5\Phi_0^2$) in the (π,π) direction. $U=4t$, $T=t/6$ at quarter-filling.

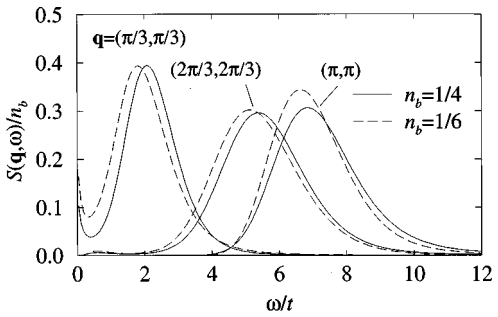

FIG. 15. Scaling of $S(\mathbf{q},\omega)$ with boson density in the (π,π) direction. The solid (dashed) lines are $S(\mathbf{q},\omega;n_h)/n_h$ for 9 (6) bosons on a 6×6 lattice. $\beta t=6$, $U=4t$, $\langle\Phi^2\rangle=0.5\Phi_0^2$.

should be a superfluid at the temperature and densities considered here, and therefore should possess well-defined phonon excitations. We see sharp phonon peaks in the density excitation spectrum, for instance, at wave vector $\mathbf{q}=(\pi/3,\pi/3)$. These long-lived phonon excitations of the superfluid phase do not survive the coherence-breaking effect of the gauge-field interactions. We find only broad peaks in $S(\mathbf{q},\omega)$ in the presence of strong random flux.

Another effect of the presence of the gauge field is a reduction in the bandwidth of the density excitations. This might be expected because the gauge-field interaction tends to increase the compressibility of the system. Indeed, we see that the center of the (π,π) peak is pulled in from $7.6t$ to $6.8t$.

We also see that the dynamic structure factor has a simple scaling with the hole density (Fig. 15): $S(\mathbf{q},\omega;n_h)=n_hS^0(\mathbf{q},\omega)$ holds for $n_h=0.1$–0.3. This is natural in a model of degenerate bosons where the boson density is equal to the hole density.

We will now compare our results with numerical results on the full t-J model.[10,11] It should be noted that, although we expect the electron density excitations of the t-J model to be dominated by its holon component, there is no quantitative equivalence between the structure factors of the t-J model and our boson-only model. Nevertheless, we argue that the dynamic structure factor of our model has qualitative similarities with that of the t-J model. For instance, the absence of sharp peaks in the dynamic structure factor is also found in the t-J model. An obvious similarity, built into our boson model *a priori*, is the lack of any structure indicating scattering across a Fermi surface at $q=2k_F$. Another feature is the scaling of dynamic structure factor with the hole density as found in Ref. 11.

We find that $S(\mathbf{q},\omega)$ along the (π,π) direction agrees well with an exact diagonalization study of the t-J model at a similar hole density, as shown in Fig. 16. (We have used a moderate rescaling of the hopping energy: $t=0.9t_0$ where t_0 is the hopping energy in the t-J model.) The area under $\mathbf{q}=(\pi/3,\pi/3)$ peak is larger in our model than in the t-J model. We believe that, as in the case of the static structure factor, this discrepancy can be improved with if we use a stronger on-site repulsion. However, the structure factor does not agree with the t-J model along the $(\pi,0)$ direction. It might be that the spectrum of the holes at zero temperature is qualitatively different from the simple tight-binding spectrum that we have assumed here. It should also be noted that

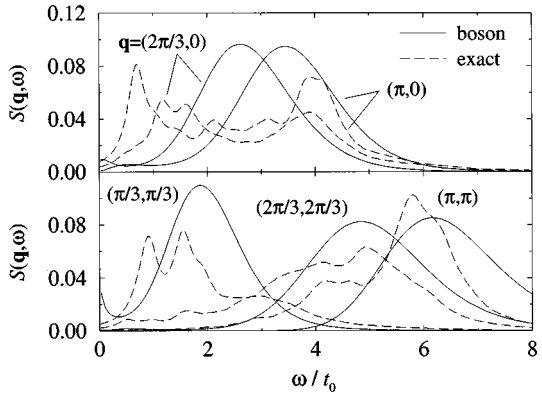

FIG. 16. Dynamic structure factor. Solid lines denote our Monte Carlo results for 6×6 lattice with nine bosons at $\beta t=6$ with $t=0.9t_0$. $\langle\Phi^2\rangle=0.5\Phi_0^2$ and $U=4t$. Dashed lines denote exact diagonalization results (Ref. 11) for four holes in an 18-site cluster with $t_0/J=2.5$.

we have neglected the spinon contribution in this comparison with results of the electronic structure factor calculated in diagonalization studies.

VIII. CONCLUSION

In summary, we have studied a degenerate Bose system which remains metallic below its degeneracy temperature due to elastic scattering with random and quasistatic gauge fields. In the path-integral picture, the bosons retrace their paths in the limit of strong gauge fluctuations in order to avoid the quantum frustration due to the fluctuating gauge field. We have demonstrated that many features of these ''Brinkman-Rice bosons'' indeed mimic the behavior of the full t-J model and the normal state of the cuprate superconductors. These features include the linear-T dependence of the longitudinal scattering rate and a charge excitation spectrum which consists of broad incoherent structures. This model itself has a strongly suppressed response to external magnetic fields, hinting that the behavior of the system as measured in Hall and magnetoresistance experiments have to understood in terms of a separate mechanism.

It would also be interesting to understand the behavior of the system in the zero-temperature limit. Although the limit of infinite gauge fluctuations (i.e., a uniform flux distribution on a lattice) would strictly forbid any world lines to wrap around periodic boundaries, one may consider the case of weaker gauge fluctuations in the zero-temperature limit and ask whether there is a critical value of $\langle\Phi^2\rangle$ below which the system is a superfluid at zero temperature. This will involve a study of the system at very low temperatures near a quantum critical point. This is beyond the scope of this paper.

ACKNOWLEDGMENTS

We thank Wolfgang von der Linden for sending us his MaxEnt code and for many helpful correspondences. We also thank W. Putikka, R. Eder, and S. Maekawa for sending us their data for comparison. We acknowledge helpful conversations with J. T. Chalker, S. M. Girvin, D. H. Lee, E. Sorensen, X.-G. Wen, and S. C. Zhang. This work was supported by the NSF MRSEC program (DMR 94-0034), NEC (D.H.K.) and EPSRC/NATO (D.K.K.L.).

APPENDIX: OPERATOR AVERAGES

In this appendix, we discuss the evaluation of operator averages. In the path-integral representation of the partition function, world-line configurations are sampled according to a distribution proportional to $\exp(-S_B^0-S_2)$. In our Monte Carlo scheme, we discretize the imaginary-time interval β into M segments of length $\Delta\tau$, and we define a world-line configuration by the boson coordinates at these discrete time points: $\{R_0,R_1,R_2,\ldots,R_M=P(R_0)\}$. [$R_m$ denotes the coordinates of the N bosons at mth time slice: $R_m=(\mathbf{x}_1^{(m)},\ldots,\mathbf{x}_N^{(m)})$, and R_M is a permutation of the coordinates of R_0.]

The configurations are sampled according to the probability:

$$\mathcal{P}(\{R\})=\frac{1}{\mathcal{N}}e^{-S_2(\{R\})}\prod_{m=0}^{M-1}\rho_{\Delta\tau}(R_m,R_{m+1}), \tag{A1}$$

where $\mathcal{N}$ is a normalization constant, and $\rho_{\Delta\tau}(R,R')$ is the short-time (high-temperature) density matrix in the absence of gauge fields. It is given by

$$\begin{aligned}\rho_{\Delta\tau}(R,R')&=\langle R|e^{-\Delta\tau(H_K^0+H_U)}|R'\rangle\\&\simeq\langle R|e^{-(1/2)\Delta\tau H_U}e^{-\Delta\tau H_K^0}e^{-(1/2)\Delta\tau H_U}|R'\rangle\\&=\langle R|e^{-\Delta\tau H_K^0}|R'\rangle e^{-(1/2)\Delta\tau(\tilde{H}_U(R)+\tilde{H}_U(R'))},\end{aligned} \tag{A2}$$

with $\tilde{H}_U(R)=\langle R|H_U|R\rangle$, and

$$H_K^0=-t\sum_{\langle ij\rangle}(b_i^\dagger b_j+\text{H.c.}), \tag{A3}$$

$$H_U=\frac{U}{2}\sum_i n_i(n_i-1). \tag{A4}$$

The error involved in this approximation of the density matrix is $O(\Delta\tau^3)$.

Measurements which depend only on particle positions are simple to evaluate in this path-integral representation. The expectation value of such a measurement $\mathcal{O}$ is given by

$$\langle\mathcal{O}\rangle=\text{Tr}[\mathcal{O}(R_0,R_1,R_2,\ldots)\mathcal{P}(R_0,R_1,R_2,\ldots)], \tag{A5}$$

where $\mathcal{O}(\{R\})$ is the measured value for the world-line configuration $\{R\}$, and the trace is taken over all such configurations.

Averages of operators which are nonlocal in position space are more cumbersome to evaluate. An example is the kinetic energy:

$$\langle H_K\rangle = -t\sum_{\langle ij\rangle}\langle (e^{ia_{ij}}b_i^\dagger b_j + \text{H.c.})\rangle. \tag{A6}$$

The gauge field a_{ij} is defined on the link between the neighboring sites i and j. The Peierls factor closes the gap in the imaginary-time loop caused by the action of kinetic energy operator. Inserting the operator H_K in the imaginary-time slice between the $m=0$ and 1, it can be shown that the kinetic energy can be evaluated as

$$\begin{aligned}\langle H_K\rangle &= \mathrm{Tr}\left[\frac{\langle R_0|H_K^0\mathcal{U}_{\Delta\tau}|R_1\rangle}{\langle R_0|\mathcal{U}_{\Delta\tau}|R_1\rangle}\mathcal{P}(\{R\})\right]\\ &= \mathrm{Tr}\left[\frac{\langle R_0|H_K^0 e^{-\Delta\tau H_K^0}|R_1\rangle}{\langle R_0|e^{-\Delta\tau H_K^0}|R_1\rangle}\right.\\ &\quad\left.\times e^{(1/2)\Delta\tau(\tilde{H}_U(R_0)-\tilde{H}_U(KR_0))}\mathcal{P}(\{R\})\right],\end{aligned} \tag{A7}$$

where $\tilde{H}_U(KR)$ is defined by $H_U\{H_K^0|R\rangle\} \equiv \tilde{H}_U(KR)\{H_K^0|R\rangle\}$, and $\mathcal{U}_{\Delta\tau}$ is the short-time evolution operator:

$$\mathcal{U}_{\Delta\tau} = e^{-(1/2)\Delta\tau H_U}e^{-\Delta\tau H_K^0}e^{-(1/2)\Delta\tau H_U}. \tag{A8}$$

[1] D.K.K. Lee, D.H. Kim, and P.A. Lee, Phys. Rev. Lett. **76**, 4801 (1996).

[2] B. Batlogg, H.Y. Hwang, H. Takagi, R.J. Cava, H.L. Kao, and J. Kwo, Physica C **235-240**, 130 (1994).

[3] For a review, see N.P. Ong, Y.F. Yan, and J.M. Harris, in *Proceedings of the CCAST Symposium on High-T_c Superconductivity and the C_{60} Family, Beijing 1994* (Gordon and Breach, New York, 1995).

[4] J. Orenstein, G.A. Thomas, A.J. Millis, S.L. Cooper, D.H. Rapkine, T. Timusk, L.F. Schneemeyer, and J.V. Waszczak, Phys. Rev. B **42**, 6342 (1990).

[5] F. Gao, D.B. Romero, D.B. Tanner, J. Talvacchio, and M.G. Forrester, Phys. Rev. B **47**, 1036 (1993).

[6] D.B. Romero, C.D. Porter, D.B. Tanner, L. Forro, D. Mandrus, L. Mihaly, G.L. Carr, and G.P. Williams, Phys. Rev. Lett. **68**, 1590 (1992).

[7] J.M. Harris, Y.F. Yan, P. Matl, N.P. Ong, P.W. Anderson, T. Kimura, and K. Kitazawa, Phys. Rev. Lett. **75**, 1391 (1995).

[8] P.W. Anderson, Science **235**, 1196 (1987).

[9] W.O. Putikka, R.R.P. Singh, R.L. Glenister, and H. Tsunetsugu, Phys. Rev. Lett. **73**, 170 (1994).

[10] T. Tohyama, P. Horsch, and S. Maekawa, Phys. Rev. Lett. **74**, 980 (1995).

[11] R. Eder, Y. Ohta, and S. Maekawa, Phys. Rev. Lett. **74**, 5124 (1995).

[12] L.B. Ioffe and A.I. Larkin, Phys. Rev. B **39**, 8988 (1989).

[13] P.A. Lee and N. Nagaosa, Phys. Rev. B **46**, 5621 (1992).

[14] J.M. Wheatley and T.M. Hong, Phys. Rev. B **43**, 6288 (1991).

[15] J.M. Wheatley and A.J. Schofield, Int. J. Mod. Phys. B **6**, 665 (1992).

[16] M. Ubbens, P.A. Lee, and N. Nagaosa, Phys. Rev. B **48**, 13 762 (1993).

[17] M.U. Ubbens and P.A. Lee, Phys. Rev. B **49**, 13 049 (1994).

[18] L.B. Ioffe and V. Kalmeyer, Phys. Rev. B **44**, 750 (1991).

[19] X.G. Wen and P.A. Lee, Phys. Rev. Lett. **76**, 503 (1996).

[20] M. Yu. Reizer, Phys. Rev. B **40**, 11 571 (1989); **44**, 5476 (1991).

[21] R. Hlubina, W.O. Putikka, T.M. Rice, and D.V. Khveshchenko, Phys. Rev. B **46**, 11 224 (1992).

[22] However, high-temperature series studies of the gauge field model[21] have found that at least the thermodynamic properties of the t-J model are well described by the gauge-field model within the Gaussian approximation.

[23] See, for example, R.P. Feynman, *Statistical Mechanics* (Addison Wesley, Reading, 1972), Chap. 11.

[24] J.A. Hertz, Phys. Rev. B **18**, 197 (1978).

[25] E.L. Pollock and D.M. Ceperley, Phys. Rev. B **36**, 8343 (1987).

[26] N. Trivedi, in *Computer Simulations in Condensed Matter Physics V*, edited by D.P. Landau, K.K. Mon, and H.B. Schüttler, (Springer-Verlag, Heidelberg, 1993).

[27] W.F. Brinkman and T.M. Rice, Phys. Rev. B **2**, 1324 (1970).

[28] R. Oppermann and F. Wegner, Z. Phys. B **34**, 327 (1979).

[29] C. Pryor and A. Zee, Phys. Rev. B **46**, 3116 (1992).

[30] A. Barelli, R. Fleckinger, and T.A.L. Ziman, Phys. Rev. B **49**, 3340 (1994).

[31] G. Gavazzi, J.M. Wheatley, and A.J. Schofield, Phys. Rev. B **47**, 15 170 (1993).

[32] N. Nagaosa and P.A. Lee, Phys. Rev. B **45**, 966 (1992).

[33] M.V. Feigelman, V.B. Geshkenbein, L.B. Ioffe, and A.I. Larkin, Phys. Rev. B **48**, 16 641 (1993).

[34] E. Fradkin, *Field Theories of Condensed Matter Systems* (Addison Wesley, Redwood City, 1991), Sec. 10.9.

[35] D.M. Ceperley and E.L. Pollock, Phys. Rev. B **39**, 2084 (1989).

[36] J.M. Wheatley, Phys. Rev. B **41**, 7301 (1990).

[37] In Ref. 14, Wheatley and Hong have defined a ''coherence temperature'' $T_{\rm coh}$ in a similar way as our T_D. In their case of bosons coupled to dissipative bath, it was argued that $T_{\rm coh}$ is pushed down to zero.

[38] M. Wallin, E.S. Sorensen, S.M. Girvin, and A.P. Young, Phys. Rev. B **49**, 12 115 (1994).

[39] G.G. Batrouni, B. Larson, R.T. Scalettar, J. Tobochnik, and J. Wang, Phys. Rev. B **48**, 9628 (1993).

[40] J. Skilling, in *Maximum Entropy and Baysian Methods* (Kluwer Academic, Dordrecht, 1989), p. 45.

[41] J.E. Gubernatis, M. Jarrell, R.N. Silver, and D.S. Sivia, Phys. Rev. B **44**, 6011 (1991).

[42] W. von der Linden, Appl. Phys. A **60**, 155 (1995).

[43] J. Jaklic and P. Prelovsek, Phys. Rev. B **52**, 6903 (1995).

[44] P.W. Anderson (unpublished).

[45] H. Fukuyama, H. Ebisawa, and Y. Wada, Prog. Theor. Phys. **42**, 494 (1969).

[46] Y.C. Chen and T.K. Lee, Phys. Rev. B **51**, 6723 (1995).